NJC

Cite this: *New J. Chem.*, 2012, **36**, 86–96

www.rsc.org/njc

PAPER

Molecular structure and acid/base properties of 1,2-dihydro-1,3,5-triazine derivatives†

Vjekoslav Štrukil,[a] Ivica Đilović,[b] Dubravka Matković-Čalogović,[b] Jaan Saame,[c] Ivo Leito,[c] Primož Šket,[de] Janez Plavec[def] and Mirjana Eckert-Maksić*[a]

Received (in Montpellier, France) 8th July 2011, Accepted 4th October 2011
DOI: 10.1039/c1nj20595a

It is shown that guanidine and its *N,N*-dimethyl-derivative react with substituted carbodiimides, affording hitherto unknown 1,2-dihydro-1,2,3-triazine derivatives. The structures of three novel compounds of this type and their perchlorate salts were elucidated by spectroscopic (IR, ^{1}H and ^{13}C NMR and ^{15}N solid-state NMR) and X-ray diffraction methods. The acid/base properties were also determined experimentally and by using DFT calculations with the B3LYP functional. The most basic compound was found to be dihydrotriazine **3**, the basicity of which with the pK_a value of 23.3 is of the same order of magnitude as that of tetramethylguanidine. Acidity measurements revealed that all the compounds studied are very weak acids with pK_a values in the range of 25.8–30.8 pK_a units in acetonitrile.

Introduction

Dihydrotriazine derivatives comprising a variety of substituents have been extensively studied in the past due to their broad biological activity. Some of these compounds have been used as antibacterial,[1] anti-inflammatory,[2] antimalarial,[3] anti-diabetic[4] and antitumor[5] agents (Scheme 1).

Other successful applications include use as herbicides,[6] insecticides[7] and corrosion inhibitors.[8] Consequently, their syntheses and the evaluation of their biological activity continue to attract considerable attention.[9] In the course of our ongoing project on the design and reactivity of strong guanidine bases,[10] we became interested in exploring the possibility of preparing some specifically substituted dihydrotriazines using guanidine derivatives and carbodiimides as reactants. This approach, as well as the reaction of biguanide derivatives and carbodiimides, has been extensively explored in the past. In all the reports published so far, only the formation of melamine or isomelamine derivatives was reported.[11–13] The reaction was proposed to proceed through the primary addition of the reactants, followed by the cyclization of the resulting intermediate triguanide, with the loss of amine, to the heterocyclic end-product.[11] However, although this approach to melamine and isomelamine derivatives has been known for a long time, no thorough study of a reaction mechanism and a structure of the so obtained products has been published as yet.[11,12] Therefore, we considered it of interest to address some of these questions in the present work. Furthermore, an additional focus of our interest in the properties of dihydrotriazines concerned their acid–base properties. Namely, due to the presence of guanidine-type subunits in their molecular framework, they are expected to exhibit basicity of a similar order of magnitude as guanidine or biguanide derivatives.[14]

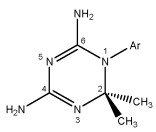

Scheme 1 The structure of cycloguanil, an antimalarial 1,2-dihydrotriazine inhibitor of dihydrofolate reductase (Ar = 4-ClC_6H_4).[3]

Herewith, we report on the synthesis and structural features of three novel 1,2-dihydro-1,3,5-triazine derivatives, namely **1–3** (Scheme 2). It should be noted that they differ from previously reported members of this family of compounds by the presence of the *exo*-cyclic imino group at ring position 2. We were particularly interested in establishing the structure of compound **1**, for which the isomelamine geometry (see Scheme 5) from UV spectral analysis was previously proposed.[11,12] Our second aim in this work was to evaluate their basicity and acidity

[a] *Ruđer Bošković Institute, Bijenička cesta 54, 10000 Zagreb, Croatia. E-mail: mmaksic@emma.irb.hr; Fax: +385-1-4680-195; Tel: +385-1-4680-197*
[b] *Faculty of Science, Department of Chemistry, Horvatovac 102A, 10000 Zagreb, Croatia*
[c] *University of Tartu, Institute of Chemistry, Ravila 14a, 50411 Tartu, Estonia*
[d] *Slovenian NMR Centre, National Institute of Chemistry, Hajdrihova 19, SI-1000 Ljubljana, Slovenia*
[e] *EN-FIST Centre of Excellence, Dunajska 156, SI-1000 Ljubljana, Slovenia*
[f] *Faculty of Chemistry and Chemical Technology, University of Ljubljana, Askerceva cesta 5, SI-1000 Ljubljana, Slovenia*

† Electronic supplementary information (ESI) available: Spectra, X-ray CIF files, tables of bond length, angles and Cartesian coordinates of the optimized structures. CCDC 830994–830998. For ESI and crystallographic data in CIF or other electronic format see DOI: 10.1039/c1nj20595a

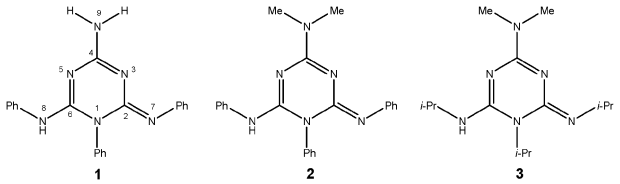

Scheme 2 The 1,2-dihydro-1,3,5-triazine derivatives **1–3** studied in this work.

experimentally by employing quantum chemical calculations. This is of considerable importance since due to the presence of *exo*-cyclic imino- and amino-type nitrogen atoms, they are expected to have the ability either to donate or accept a proton, *i.e.*, to act as either an acid or a base (Scheme 2). In addition, the results of a computational study of the effect of *p*-substituents in aryl-substituted species on the protonation energies, with the goal of designing potentially stronger acids/bases belonging to this class of compounds, will be presented. To the best of our knowledge, this has been the first comprehensive study of the structural features and acid/base properties of 1,2-dihydro-1,3,5-triazine derivatives so far.

Results and discussion

Synthesis and characterization of products

Compounds **1–3** were prepared in an excellent yield by applying a modified one-pot procedure based on a protocol reported earlier by Kurzer and Pitchfork.[11] Guanidine (**4**) or *N*,*N*-dimethylguanidine (**5**) was first treated with two equivalents of *N*,*N*′-diphenylcarbodiimide (**6**) in refluxing THF (Scheme 3), affording the phenyl derivatives **1** and **2** in moderate yields (60% and 51%, respectively), accompanied by the corresponding biguanide derivative and *N*,*N*′,*N*″-triphenylguanidine (**8**) (Fig. S1, ESI†; Scheme 4). This suggests that the aniline molecule liberated during cyclization competes with the *in situ* formed biguanide derivative for *N*,*N*′-diphenylcarbodiimide (**6**), yielding by-product **8**. To increase the yield, the reaction was repeated using three equivalents of *N*,*N*′-diphenylcarbodiimide (**6**), which led to a complete consumption of the biguanide intermediate and an increase in the isolated yield of the cyclic product to 98% (**1**) and 94% (**2**), respectively (Fig. S2, ESI†). After removing the solvent, the main product was isolated by suspending the crude reaction mixture in diethylether followed by filtration (**1** and **2**). In the case of the isopropyl derivative **3**, the reaction was carried out using a 1 : 2 ratio of **5** and **7**, and a pure product was isolated by high-vacuum distillation in 80% yield. Moreover, no *N*,*N*′,*N*″-triisopropylguanidine (**9**) was observed, presumably due to the lower reactivity of dialkylcarbodiimide **7** (R_2 = *i*-Pr) and high volatility of isopropylamine (bp 32 °C) under the applied experimental conditions. Another important observation is that an intermediate triguanide derivative could not be identified in any of the reactions studied in this work, which is in accordance with the available literature studies.[11,12]

This confirms the previous proposition[11,12] that an intermediately formed triguanide derivative undergoes spontaneous cyclization accompanied by the elimination of amine R_2NH_2 (aniline in the reaction of *N*,*N*′-diphenylcarbodiimide (**6**) or isopropylamine when *N*,*N*′-diisopropylcarbodiimide (**7**) is used). From a mechanistic point of view, two modes of cyclization to 1,2-dihydrotriazines could be envisaged (Scheme 4): one starting directly from the triguanide moiety **10** (path A) or from its ring tautomer intermediate **11**, which is formed by a nucleophilic attack of the lone pair at the imino nitrogen N1 to the carbon atom C6 in triguanide **10**, followed by the elimination of the R_2NH_2 molecule (path B). This type of tautomerism is well known from, *e.g.*, sugar chemistry.[15] More recently, chain–ring tautomerism, which, in fact, corresponds to thermally allowed 6π-electrocyclization, has also been invoked to explain the mechanism of the cyclization of some unsaturated hetero chains of the oligonitrile type into 1,2-dihydro-1,3,5-triazine derivatives.[16]

However, in this work, we could not confirm the presence of these intermediates experimentally due to their obvious instability. Therefore, we calculated the energies of both types of tautomers for the model compounds in which R_1 and R_2 groups were replaced by methyl groups, using the B3LYP/6-311 + G(d,p)//B3LYP/6-31G(d,p) method. In addition to the gas phase, calculations were carried out in THF as the solvent. The geometries of the fully optimized species are shown in Fig. S3 and Table S1 (see ESI†) and the computed energies are listed in Table 1. A glance at the calculated energies in Table 1 clearly shows that the open-chain and cyclic tautomers **10** and **11** are of similar stability, with the latter being slightly more stable in THF (by 1.07 kcal mol^{-1}). Thus, based on these data, albeit qualitative, we presume that path B would be favored.

The 1,2-dihydrotriazine products were fully characterized by elemental analysis and spectroscopic methods (IR, HRMS, ^1H and ^{13}C solution and ^1H, ^{13}C and ^{15}N solid-state NMR).

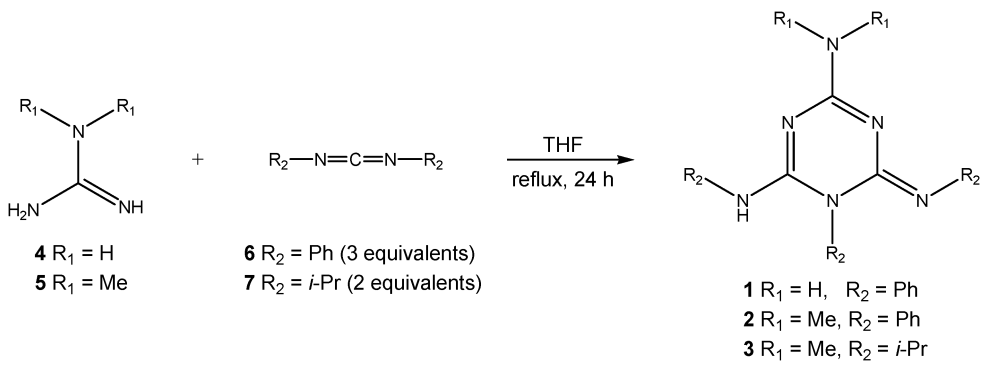

Scheme 3 Synthesis of triazines **1–3**.

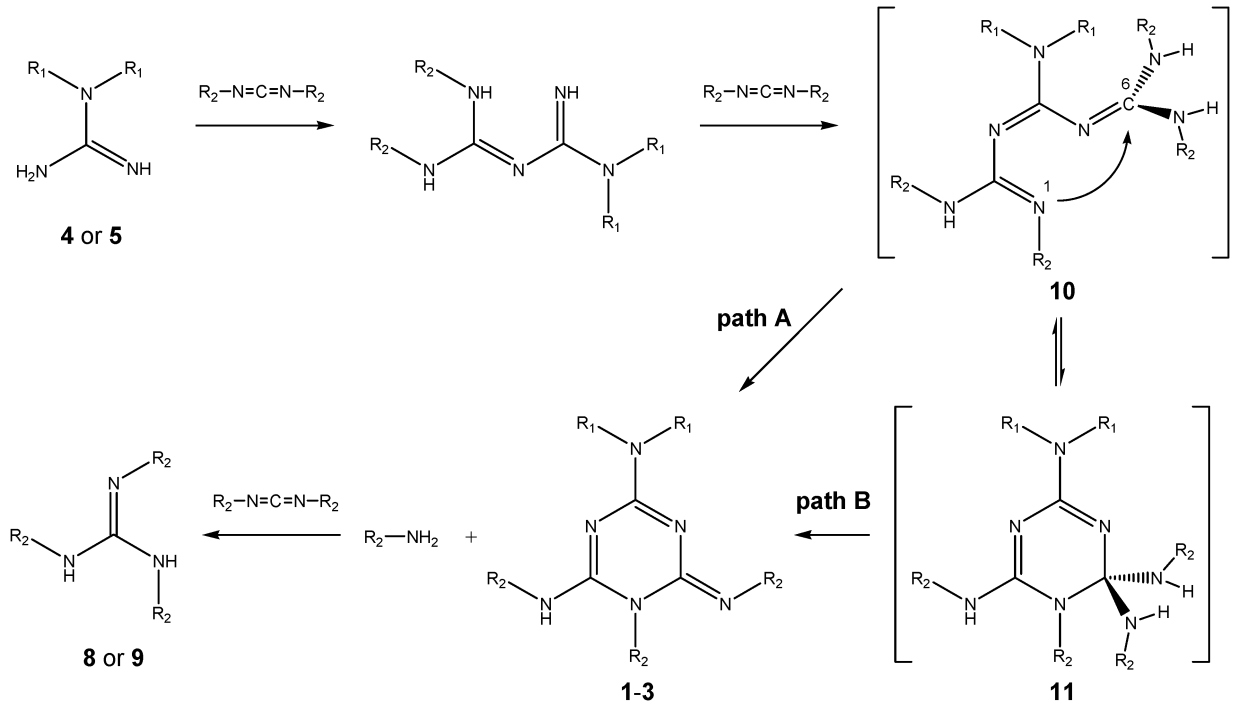

Scheme 4 Possible mechanisms of the formation of 1,2-dihydro-1,3,5-triazine derivatives **1–3** (R_1 = H or Me, R_2 = Ph or *i*-Pr).

Table 1 Single point B3LYP/6-311+G(d,p)//B3LYP/6-31G(d,p) and CPCM/B3LYP/6-31G(d,p) energies in the gas phase and THF solution for open-chain and cyclic tautomers **10** and **11**, respectively

Structure[a]	E_{el}/a.u.	E_{ZPV}/a.u.	E_{tot}/a.u.	E_{rel}/kcal mol^{-1}
Gas phase				
10	−739.06485	0.32223	−738.74262	0.00
TS	−739.04652	0.32210	−738.72442	11.42
11	−739.06342	0.32486	−738.73856	2.55
THF solution				
	ΔG_{solv}/kcal mol^{-1}		E_{rel}^{solv}/kcal mol^{-1}	
10	11.61		0.00	
TS	8.81		8.62	
11	7.99		−1.07	

[a] R_1 = R_2 = CH_3, see Scheme 4. TS corresponds to the transition structure for chain-tautomer cyclization.

The structures of compounds **1** and **2** were ultimately confirmed by X-ray diffraction analysis. In the mass spectra, all three compounds gave the expected molecular ion [MH^+] along with some fragment ions. The proposed structures were supported by analysis of the solution and solid-state NMR spectra. For instance, taking the ^{1}H NMR spectra in the solution of compound **3** as an example, we observe a broad doublet at 6.15 for the C–N*H* proton, a singlet for the protons of the N–CH_3 group at 2.96 ppm, three multiplets for the N–C*H* protons in the range of 3.96–4.76 ppm and three doublets for the CH–CH_3 protons in the range of 0.96–1.41 ppm. The corresponding ^{13}C NMR spectrum in solution displays three signals between 159.2–148.2, three signals between 45.3–42.8 ppm, one signal at 35.5 ppm and three signals between 24.5–19.4 ppm assigned to the ring carbon atoms, *C*H carbon atoms of three chemically different isopropyl groups, N–CH_3 and C–CH_3 carbon atoms, respectively.

Similar chemical shifts for carbon atoms have been observed in the solid state as well (Fig. 1). The ^{1}H and ^{13}C NMR spectra of triphenyl derivatives **1** and **2** (see the Experimental section) in solution, as well as in the solid state (Fig. S4–S7 and S19–S22 in ESI†), are also fully consistent with the 1,2-dihydro-1,3,5-dihydrotriazine structures. Notably, the signals for the N*H* proton in the ^{1}H NMR spectra of **1** and **2**, taken in DMSO, appear in the same region (7.61 ppm in **1** and 7.75 ppm in **2** in DMSO), thereby confirming that the imino proton is in the same chemical environment in both compounds (Fig. S4 and S6 in ESI†).

Furthermore, in the ^{15}N CP-MAS NMR spectra, the most upfield signals between −290 and −300 ppm indicate the presence of the amino/dimethylamino group attached to the C4 atom (Fig. 2).

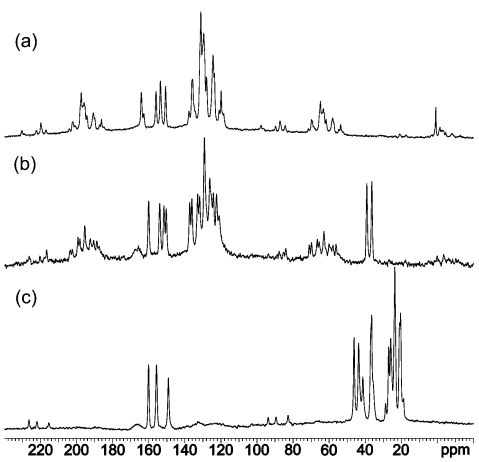

Fig. 1 ^{13}C CP-MAS NMR spectra of compounds **1** (a), **2** (b) and **3** (c).

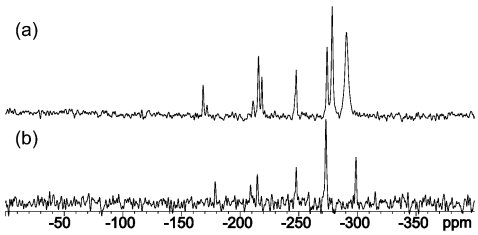

Fig. 2 ^{15}N CP-MAS NMR spectra of compounds **1** (a) and **2** (b).

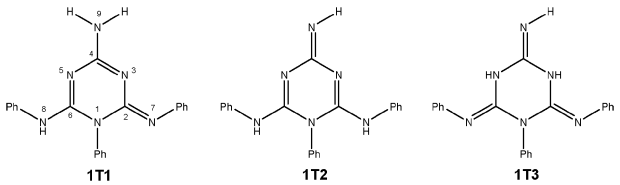

Scheme 5 Possible tautomeric structures of molecule **1**. **1T1**-imino, **1T2**-quinoid and **1T3**-isomelamine structures.

Even more importantly, the signals for N3 and N5 atoms have different chemical shifts. In the case of **1**, this excludes the existence of the quinoid and isomelamine structures **1T2** and **1T3** (Scheme 5), in which we would expect to observe a single resonance for both atoms due to the symmetry of the molecule. In order to obtain insights into the intrinsic stabilities of tautomers **1T1–1T3** of compound **1**, their energies were calculated using the B3LYP/6-311 + G(d,p)//B3LYP/6-31G(d) method. At this level of theory, tautomer **1T1** was found to be more stable than **1T2** and **1T3** by 15.2 and 11.6 kcal mol^{-1}, thus being in accordance with NMR data (see Table S3 for energies in ESI†).

Finally, an interesting feature observed in the ^{15}N CP-MAS NMR spectrum of compound **1** concerns the presence of a larger number of signals than in compound **2**, indicating that two molecules are present in the asymmetric unit of compound **1**, while a single molecule is present in the asymmetric unit of compound **2** in the solid state. This, as will be shown below, was confirmed by X-ray diffraction data.

X-Ray structure determination of 1 and 2

The crystal and molecular structures of the methanol solvate of compound **1** (**1**·0.5 MeOH) and compound **2** were determined by the single crystal X-ray diffraction method (Table 3). The asymmetric unit of **1**·0.5 MeOH consists of two different conformers of **1** (**1a** and **1b**) and a methanol molecule, while that of **2** contains a single molecule (Fig. 3 and 4). The selected bond lengths are given in Table 2. Their perusal clearly indicates that imino tautomer **1T1** is present in both compounds. The carbon–nitrogen bond distances within the triazine ring range

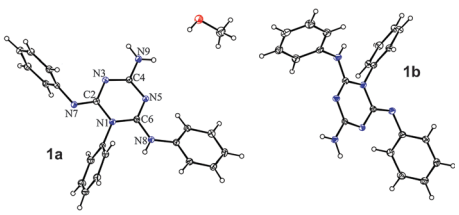

Fig. 3 ORTEP drawing of **1**·0.5 MeOH. Thermal ellipsoids are at the 30% probability level.

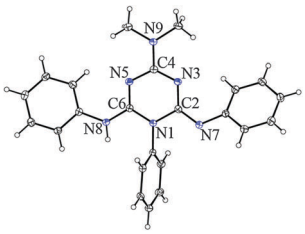

Fig. 4 ORTEP drawing of **2**. Thermal ellipsoids are at the 30% probability level.

Table 2 Selected bond lengths (Å) for **1**·0.5 MeOH and **2**[a]

Bond	1a	1b	2
N1–C2	1.416(2)	1.419(2)	1.433(2)
N1–C6	1.374(2)	1.372(2)	1.371(2)
C2–N3	1.360(2)	1.370(2)	1.354(2)
N3–C4	1.331(2)	1.329(2)	1.328(2)
C4–N9	1.325(2)	1.333(2)	1.346(2)
C4–N5	1.367(2)	1.366(2)	1.362(2)
N5–C6	1.302(2)	1.317(2)	1.308(2)
C2–N7	1.292(2)	1.287(2)	1.292(2)
C6–N8	1.359(2)	1.343(2)	1.361(2)
N1–Ph	1.447(2)	1.444(2)	1.444(2)
N7–Ph	1.423(2)	1.416(2)	1.411(2)
N8–Ph	1.418(2)	1.433(2)	1.424(2)

[a] For numeration of atoms see Fig. 3 and 4.

from 1.302(2) Å to 1.433(2) Å, and are also in agreement with this tautomeric form, albeit with extensive delocalization. Such delocalized C=N bonds were also reported for the structurally related 1,6-dihydro-1,3,5-triazine derivative.[17]

It is important to note that the NH_2 group (NMe_2 in **2**) is practically coplanar with the triazine moiety, thus enabling effective delocalization of the nitrogen lone pair in the triazine ring. Another notable feature concerns the difference in the length of the exocyclic C2–N7 and C6–N8 bonds. While the length of the C2–N7 bond (1.292(2) Å and 1.287(2), 1.292(2) Å in **1a**, **1b**, and **2**, respectively) corresponds to a typical C=N double bond, the C6–N8 bond (ranging from 1.343(2) to 1.361(2) Å) has a value closer to a typical Nsp^2–Csp^2 single bond, such as in ref. 18.

In the crystal structure of **1**·0.5 MeOH, the two conformers are connected by hydrogen bonds of the type N–H···N (2.912(2) and 3.053(2) Å), forming a ring that can be described by the graph-set notation $R_2^2(8)$.

The methanol molecule is a donor in the hydrogen bond O–H···N (2.915(2) Å) to molecule **1a** and is an acceptor of a weak hydrogen bond C–H···O from a neighboring **1a** molecule (Fig. 5). Such supramolecular assemblies are interconnected in the crystal structure by weak interactions of the type C–H···O, C–H···N, C–H···π and N–H···π.

In contrast, packing in the crystal structure of **2** is achieved through weak interactions, mostly of the C–H···π type. The protonated nitrogen atom N8 is sterically hindered and not involved in hydrogen bonding.

The effect of protonation on the molecular structure of 1–3

In order to confirm the site of proton attack and to obtain insights into the effect of protonation on the structure of the

Table 3 General and crystal data, summary of intensity data collection and structure refinement

	1·0.5 MeOH	**2**	**2**·$HClO_4$	**3**·$HClO_4$
Empirical formula	$2(C_{21}H_{18}N_6)$, CH_4O	$C_{23}H_{22}N_6$	$C_{23}H_{23}N_6$, ClO_4	$C_{14}H_{29}N_6$, ClO_4
Formula weight	740.87	382.47	482.92	380.88
Crystal system, space group	Monoclinic, *P* $2_1/c$	Orthorhombic, *P bca*	Orthorhombic, *P* $2_12_12_1$	Monoclinic, *P* $2_1/c$
Unit cell dimensions (Å, °)				
a	14.1696(2)	19.0976(8)	6.9133(5)	9.4056(10)
B	17.3971(4)	9.1823(3)	15.5643(12)	9.3787(9)
c	15.0518(3)	21.9471(8)	20.7086(14)	22.2736(18)
α	90.00	90.00	90.000	90.00
β	91.7700(20)	90.00	90.000	98.682(7)
γ	90.00	90.00	90.000	90.00
Volume/Å^3	3708.65(12)	3848.6(2)	2228.3(3)	1942.3(3)
Z	4	8	4	4
D_{calc}/g cm^{-3}	1.327	1.320	1.440	1.303
T/K	100(2)	100(2)	150(2)	110(2)
Reflections observed/independent (R_{int})	35 085/6866 (0.0366)	12 539/3363 (0.0426)	5090/3659 (0.0297)	15 999/3799 (0.0317)
Observed reflections [$I > 2\sigma(I)$]	4991	2698	2760	3083
Goodness-of-fit on F^2	0.979	1.072	1.033	1.121
R/wR [$I > 2\sigma(I)$][a]	0.0443/0.1067	0.0454/0.0892	0.0632/0.1065	0.0488/0.1235
R/wR (all data)[b]	0.0642/0.1172	0.0642/0.0958	0.0910/0.1167	0.0624/0.1317
Flack parameter	—	—	−0.04(12)	—

[a] $R = \sum||F_o| - |F_c||/\sum F_o$, $w = 1/[\sigma^2(F_o^2) + (g_1P)^2 + g_2P]$ where $P = (F_o^2 + 2F_c^2)/3$, $S = \Sigma[w(F_o^2 - F_c^2)^2/(N_{obs} - N_{param})]^{1/2}$. [b] $wR = [\Sigma(F_o^2 - F_c^2)^2/\Sigma(F_o^2)^2]^{1/2}$.

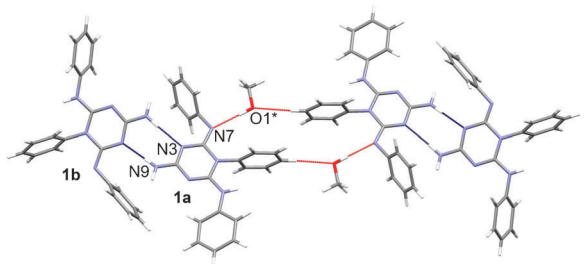

Fig. 5 A supramolecular assembly in the structure of **1**·0.5 MeOH showing molecules interconnected by hydrogen bonds (blue and red lines). Symmetry code * = 1 − *x*, −*y*, −*z*.

compounds considered, we measured the X-ray structure of the monocrystals of the perchlorate salts of **2** and **3** (Fig. 6). All attempts to prepare single crystals of the perchlorate salt of **1** suitable for X-ray measurements were unsuccessful. Therefore, in order to obtain insights into the structure of protonated **1**, its geometry was optimized using the B3LYP/6-31G(d) method. The key structural parameters of the calculated and experimentally determined structures of the protonated species, **2**·$HClO_4$ and **3**·$HClO_4$, are listed in Table 4, while the summary of all the calculated parameters and relevant parameters for the neutral molecules is presented in Tables S4–S6 in the ESI.†

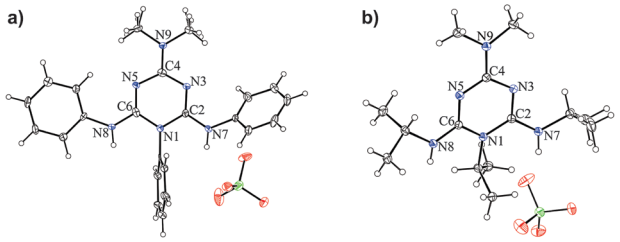

Fig. 6 ORTEP drawings of (a) **2**·$HClO_4$ and (b) **3**·$HClO_4$. The thermal ellipsoids are at the 30% probability level.

Table 4 Comparison of the single-crystal measured bond lengths of salts with the calculated distances in protonated **1–3**.[a] The geometries of the protonated species $\mathbf{1H}^+$, $\mathbf{2H}^+$ and $\mathbf{3H}^+$ were optimized at the B3LYP/6-31G(d) level of theory

	d/Å				
Bond	Theory $\mathbf{1H}^+$	Measured **2**·$HClO_4$	Theory $\mathbf{2H}^+$	Measured **3**·$HClO_4$	Theory $\mathbf{3H}^+$
N1–C2	1.401	1.397(5)	1.401	1.393(2)	1.400
N1–C6	1.402	1.401(6)	1.401	1.389(2)	1.401
C2–N3	1.317	1.304(5)	1.311	1.320(3)	1.317
N3–C4	1.349	1.376(6)	1.357	1.347(2)	1.354
C4–N9	1.336	1.318(5)	1.340	1.336(2)	1.341
C4–N5	1.349	1.350(5)	1.357	1.349(3)	1.355
N5–C6	1.317	1.307(5)	1.311	1.322(2)	1.316
C2–N7	1.343	1.352(6)	1.347	1.330(3)	1.340
C6–N8	1.343	1.333(5)	1.347	1.333(3)	1.344
N1–Ph (*i*-Pr)	1.449	1.446(5)	1.448	1.503(2)	1.505
N7–Ph (*i*-Pr)	1.432	1.437(5)	1.432	1.478(3)	1.483
N8–Ph (*i*-Pr)	1.432	1.429(6)	1.432	1.479(3)	1.484

[a] For numbering of the atoms see Scheme 2 and Fig. 6.

Before analyzing the effect of protonation on **1–3** in detail, we note that the trend of the changes in the calculated structural parameters in $\mathbf{2H}^+$ and $\mathbf{3H}^+$ closely resembles those found in the X-ray structures of their perchlorate salts. The same holds for the comparison of the experimental and calculated structures of **1** and **2** and their protonated forms with those of the corresponding perchlorate salts. This, in turn, lends credence to the structural parameters calculated for the other species studied in this work.

The most striking feature of the experimental structures of the protonated species concerns the elongation of the C2–N7 bond relative to that in the neutral molecule, confirming that protonation occurs at the N7 atom. This results in a near equalization of the exocyclic C2–N7 and C6–N8 bonds, accompanied by changes in the bond lengths within the triazine ring, which assumes a *para* quinonoid character with

Table 5 Results of basicity measurements in acetonitrile

Compd. (B)	Reference base (Rb)	pK_a (Rb)	ΔpK_a[a]	pK_a (B)	Assigned pK_a[b](B)
1	2-Cl–$C_6H_4P_1$(pyrr)	20.17	1.69	18.48	18.51
	2-Cl–$C_6H_4P_1$(dma)	19.07	0.59	18.48	
	2,6-Cl_2–$C_6H_3P_1$(pyrr)	18.56	0.00	18.56	
2	$PhP_1(dma)_2Me$	21.03	1.89	19.14	19.14
	2-Cl–$C_6H_4P_1$(pyrr)	20.17	1.01	19.16	
	2-Cl–$C_6H_4P_1$(dma)	19.07	−0.05	19.12	
3	2-Cl–$C_6H_4P_2$(dma)	24.23	1.23	23.00	23.02
	PhP_1(pyrr)	22.34	−0.72	23.06	

[a] pK_a(Rb) − pK_a(B). [b] The standard uncertainties of the pK_a values relative to the acetonitrile pK_a scale are estimated as 0.05 pK_a units (see ref. 20*e*).

the C2–N3 and N5–C6 bond lengths being close to typical Csp^2–Nsp^2 bonds.

Basicity and acidity determination

The results of basicity and acidity measurements are presented in Tables 5 and 6, respectively. Also included in Tables 5 and 6 are the reference bases and acids used in this work. The basicity and acidity of a wide range of neutral heterocyclic and acyclic nitrogen-containing compounds have been measured previously in acetonitrile by several groups,[19–21] resulting in well-defined acidity scales covering 24 orders of acidity[20*a*,*b*] and a base scale covering 28 orders of basicity,[20*c*,*d*] thus facilitating comparison of the pK_a values of the compounds studied in this work with previously measured ones.

Analysis of the results for the basicity measurements of **1–3** (Table 5) reveals that the basicity of **3** is the highest among the studied dihydrotriazines. Its pK_a value lies between those for the 2-Cl-$C_6H_4P_2$(dma) and PhP_1(pyrr) reference bases. In relation to our current interest in the basicity of guanidine compounds,[19] which, similarly to the present compounds, undergo protonation at the imino group, we note that this pK_a value is of the same order of magnitude as that of tetramethylguanidine (23.3 pK_a units)[20*f*] and 3.9 pK_a units smaller than the pK_a value of *N*,*N*′,*N*′′-tris(3-dimethylaminopropyl)guanidine, which is the most basic acyclic guanidine derivative studied so far.[19] It should be, however, emphasized that the high basicity of the latter compound is to a large extent due to the presence of cooperative intramolecular hydrogen bonds and their impact on the stabilities of the base and its conjugated acid,[19] which are not present in dihydrotriazines studied in this work. Replacement of the isopropyl groups with the electron-withdrawing phenyl rings, leading to **2** and **1**, leads to a decrease in basicity of 3.9 and 4.5 pK_a units (in acetonitrile), respectively. It is noteworthy that replacement of the amino group with the dimethylamino moiety in **1** leading to **2** causes partial cancellation of the electron-withdrawing effect of the phenyl rings, resulting in a slight enhancement of basicity.

Table 6 Results of acidity measurements in acetonitrile

Compd. (A)	Reference acid (Ra)	pK_a (Ra)	ΔpK_a[a]	pK_a (A)	Assigned pK_a[b] (A)
1	$(C_6F_5)(C_6H_5)CHCN$	26.14	0.31	25.83	25.83
	$(C_5F_4N)(C_6H_5)NH$	26.34	0.51	25.83	
2	$(C_6F_5)(C_6H_5)CHCN$	26.14	−0.47	26.61	26.6
	$(C_5F_4N)(C_6H_5)NH$	26.34	−0.32	26.66	
	(4-Me-C_6F_4)$(C_6F_5)NH$	24.94	−1.48	26.42	
3	9-C_6F_5-Fluorene	28.11	−2.7	30.8	30.8
	2,3,4,5,6-$(CF_3)_5$-Toluene	28.7	−2.1	30.8	

[a] pK_a(Ra) − pK_a(A). [b] The standard uncertainties of the pK_a values relative to the acetonitrile pK_a scale are estimated as 0.06 pK_a units for **1** and 0.2 pK_a units for **2** and **3** (see ref. 20*e*).

Comparison of the measured acidity data (Table 6) with those encompassed by the previously published acidity scale of the neutral compounds indicates that the acidity of the NH proton in **1–3** has been among the lowest measured in acetonitrile so far. Thus, the acidity of **3** is *ca.* 2 pK_a units lower than that of 9-C_6F_5-fluorene (28.11), which has the lowest acidity in the previously reported acidity scale[20*a*] and thus **3** extends the previously established pK_a scale of acidity in acetonitrile. The acidity of the respective protons in **1** and **2** is 5.0 and 4.2 pK_a units higher relative to **3**. The observed enhancement in acidity can be understood by comparing the calculated charge density distribution in the molecules considered. Due to the delocalization of electronic density on the deprotonation site into the neighboring phenyl ring in molecules **1** and **2**, the loss of the proton from this site becomes easier and the resulting anion more stabilized than in the case of **3**, where such delocalization is not possible (Tables S8–S10 in the ESI†).

Comparison of the measured and calculated pK_a values of bases **1–3** in acetonitrile

Due to the wide interest in the design of strong organic bases in synthetic work, considerable efforts have been devoted in the past to the development of practical theoretical methods capable of predicting pK_a values in organic solvents. The *a priori* estimates of the pK_a values from the first principles[22] are, unfortunately, still not feasible in larger molecules of practical interest. Therefore, it is necessary to resort to simpler models of the polarized continuum (PCM)[23] and its isodensity (IPCM) variant form.[24] We have recently demonstrated that the latter approach in conjunction with the B3LYP/6-311 + G(d,p)//B3LYP/6-31G(d) method for a large number of strong neutral nitrogen bases yields a fair correlation with the experimental pK_a values of a large number of nitrogen bases.[25]

Having measured the pK_a values of guanidines **1–3**, we decided to test the applicability of such correlations for calculating the pK_a values of these types of bases. For this purpose, we used a slightly modified approach as employed in ref. 25. Specifically, the IEF-PCM model was used for calculating solvation energies instead of the IPCM method, due to a problem in the convergence of the isodensity surfaces for several structures. The same approach was subsequently used to evaluate the effect of a series of selected substituents in the *para* position of the phenyl rings, using molecule **2** as an example. All the optimized geometries were verified to be minima by vibrational analysis at the same level of theory. The resulting internal coordinates of all the optimized species are shown in Table S11 in the ESI.† The electronic energies and Gibbs energy corrections were calculated by the B3LYP/

6-311 + G(d,p) and B3LYP/6-31G(d) methods, respectively. Zero point vibrational energies were used unscaled. pK_a values for the examined dihydrotriazines were calculated using linear eqn (1).[26]

$$pK_a(\text{calc}) = 0.617 \times GB'(B)_{AN} - 155.585 \quad (1)$$

where GB′ stands for the "reduced basicity" of the neutral base B in acetonitrile and is calculated according to eqn (2)

$$GB'(AN) = GB'(B)_{gas} + \Delta G(BH^+)_{AN} - \Delta G(B)_{AN} \quad (2)$$

where $\Delta G(BH^+)_{AN}$ and $\Delta G(B)_{AN}$ correspond to solvation energies of the protonated and neutral bases, respectively.

The parameters for eqn (1) were evaluated from the linear relationship calculated for the test set of the 57 different nitrogen bases also used in our previous calculations, which span a range of *ca.* 40 pK_a units. The calculated $GB'(B)_{AN}$ and pK_a(calc) values of the compounds considered (as bases) are summarized in Table 7.

Before considering the effect of substituents on the basicity of compound **2**, we note that the calculated pK_a values for bases **1–3** are in excellent agreement with the experimentally measured values. Analysis of the data calculated for compound **2** substituted in the *para* position of the phenyl rings shows the strong impact of the electronic properties of the substituents on basicity. As expected, the effect of strong electron-donating dimethylamino groups is the most profound, causing an increase in basicity by *ca.* 5 pK_a units. It is interesting to note that the effect of the dimethylamino group is additive; the largest contribution arises from the dimethylamino group at the phenyl ring attached to the N^7 (2.12 pK_a units), at which protonation takes place. This is followed by the contribution of the dimethylamino group at the N^1 (1.73 pK_a units) and N^8 (0.94 pK_a units) (Table 7). A somewhat weaker effect is observed for the amino substituted species, while methoxy and methyl groups increase basicity only moderately. On the other hand, substitution by the electron-accepting groups lowers basicity, with the largest effect encountered for the nitro-substituted species. To summarize, the chosen set of substituents facilitates fine-tuning of the basicity of the examined compound in the range of *ca.* 10 pK_a units. It is quite plausible that all of these species can be easily prepared. Their use in further studies could lead to fine refinement of the existing scales of basicity in the range of *ca.* 14 to 24 pK_a values.

Conclusions

One-pot synthesis of hitherto unknown 1,2-dihydro-1,2,3-triazine derivatives, starting from the corresponding guanidine and carbodiimide derivatives and their characterization using spectroscopic (IR, ^{1}H and ^{13}C solution-state and ^{13}C and ^{15}N solid-state NMR) methods, is described. The structures of two of the prepared compounds and their perchlorate salts were also confirmed by the X-ray diffraction method. This is, to the best of our knowledge, the first report on the preparation and structural determination of 1,2-dihydro-1,3,5-triazines possessing *exo*-cyclic imino group at ring position 2, thus opening a new avenue in exploring chemistry of this family of compounds. Due to the presence of exo-cyclic imino- (N7) and amino-type (N8) nitrogen atoms, the parent compounds were assumed to possess the ability either to donate or accept a proton, *i.e.*, to act as either an acid or a base. This was confirmed by measuring basicity and acidity in acetonitrile and quantum chemical calculations. The most basic species was found to be compound **3**, the basicity of which was of the same order of magnitude as that of tetramethylguanidine. Acidity measurements revealed that all the compounds studied behave like very weak acids, having pK_a values in the range of 25.8–30.8 pK_a units in acetonitrile. Finally, the pK_a values were also calculated by the IEF-PCM model employing the B3LYP/6-311 + G(d,p)//B3LYP/6-31G(d) method and were found to be in excellent agreement with the measured values, confirming high predictive power of the theoretical approach used. The same method was used to calculate the effect of a series of substituents in the *para* positions of the aromatic rings in **2**, suggesting that in this way a fine-tuning of the basicity of the examined compound in the range of *ca.* 10 pK_a units could be attained. It is quite plausible that all of these species can be easily prepared and their use in further basicity measurements could have significant impact on fine refinement of the existing scales of basicity in the range of *ca.* 14 to 24 pK_a values, and could presumably lead to new types of strongly basic organocatalysts.

Table 7 Solvation-free energies, proton affinities and calculated and experimental pK_a values of the bases **1–3** in acetonitrile (AN)[a]

Molecule	$GB(B)_{gas}$ (kcal mol^{-1})	$GB'(B)_{gas}$	$\Delta G(X)_{AN}$/kcal mol^{-1}		$GB'(B)_{AN}$/kcal mol^{-1}	pK_a(calc)	pK_a (exp)	Δ(pK_a)
			X = B	X = BH$^+$				
1	247.35	253.63	3.80	−25.18	282.61	**18.78**	**18.51**	**−0.27**
2	249.49	255.77	9.30	−18.36	283.43	**19.29**	**19.14**	**−0.15**
3	250.42	256.70	14.66	−18.50	289.86	**23.26**	**23.02**	**−0.24**
2-NO$_2$	226.77	233.05	−0.26	−42.10	274.89	**14.02**		
2-CN	230.09	236.37	1.10	−39.37	276.84	**15.23**		
2-Cl	242.59	248.87	10.82	−22.57	282.26	**18.57**		
2-F	243.97	250.25	10.41	−22.53	283.19	**19.14**		
2-Me	253.53	259.81	13.42	−12.68	285.91	**20.82**		
2-OMe	255.71	261.99	8.67	−16.43	287.09	**21.55**		
2-NH$_2$	260.28	266.56	0.27	−22.49	289.32	**22.93**		
2-NMe$_2$	264.77	271.05	13.68	−6.46	291.19	**24.08**		
2-N^7PhNMe$_2$	255.46	261.74	10.60	−14.52	286.86	**21.41**		
2-N^7,N^8PhNMe$_2$	259.37	265.65	11.92	−10.82	288.39	**22.35**		

[a] For numeration of atoms see Scheme 2.

Experimental section

Materials and methods

All reagents and solvents were purchased from commercial sources and were further purified by the standard methods, if necessary. ^{1}H and ^{13}C NMR spectra were recorded on Brucker Avance (300 and 600 MHz) spectrometers with tetramethylsilane as an internal standard, while IR spectra were obtained on an ABB Bomem MB102 spectrophotometer (CsI optics, DTGS detector, KBr pellets technique).

NMR spectra of solid samples were recorded on a Varian NMR System 600 MHz NMR spectrometer equipped with a 3.2 mm NB Double Resonance HX MAS Solids Probe. The Larmor frequencies of protons, carbon and nitrogen nuclei were 599.77 MHz, 150.83 MHz and 60.78 MHz, respectively. The ^{1}H MAS NMR spectra were externally referenced using adamantane. The ^{13}C CP-MAS NMR spectra were externally referenced using hexamethylbenzene (HMB). The ^{15}N CP-MAS NMR spectra were externally referenced using ammonium sulfate (δ −355.7 ppm regarding nitromethane at δ 0.0 ppm). Samples were spun at the magic angle at 20 kHz during ^{1}H measurement and 10 kHz during ^{13}C and ^{15}N measurements. The ^{1}H spectra were acquired using an echo pulse sequence. The repetition delay was 5 s and the number of scans was 16. The pulse sequences used for acquiring the ^{13}C and ^{15}N spectra were standard cross-polarization MAS pulse sequences with high-power proton decoupling during acquisition. The repetition delay was 5 s. The numbers of scans were between 600 and 2200 for the ^{13}C measurements and 22 000 and 27 000 for ^{15}N measurements.

HPLC analyses were performed on a Varian ProStar Instrument supplied with a UV/Vis detector using a Restek UltraIBD C18 (reversed phase) 5 μm 250 × 4.6 mm column operated at room temperature with a flow rate of 1 mL min^{-1}; gradient of 2% acetic acid (solvent A) and methanol (solvent B): 95% A + 5% B, 0–5 min; 85% A + 15% B, 5–45 min, 35% A + 65% B, 45–55 min, 5% A + 95% B, 55 min. Melting points were determined on a Kofler hot-stage apparatus and are uncorrected. Elemental analyses were performed on a Perkin Elmer 2400 Series II CHNS/O Analyzer.

Synthesis

***N,N*-Dimethylguanidine (5)**. To a freshly prepared solution of sodium methoxide in methanol (0.46 g, 0.02 mol Na in 10 cm^3 of dry methanol), *N,N*-dimethylguanidinium sulfate (2.72 g, 0.01 mol) was added under an argon atmosphere and stirred first at ambient temperature for 60 minutes and then at 50 °C for another 30 minutes. The solvent was then evaporated under vacuum, the residue treated with dry dichloromethane and filtered off over a sinter funnel. Evaporation of the remaining filtrate afforded neutral *N,N*-dimethylguanidine (**5**) as a white solid (1.60 g, 92%).

υ_{max}/cm^{-1} 3352, 1638, 1430, 1070. δ_H(600 MHz; d_6-DMSO; Me_4Si) 2.74 (6 H, s, C*H*$_3$), 4.30–4.70 (3 H, br s, N*H*). δ_C(150 MHz, d_6-DMSO; Me_4Si) 37.5, 160.0.

***N,N′*-Diphenylcarbodiimide (6)**. *N,N′*-Diphenylthiourea (0.39 g, 1.7 mmol), yellow mercury oxide (0.37 g, 1.7 mmol) and anhydrous sodium sulfate (0.24 g, 1.7 mmol) were stirred in dry dichloromethane (10 cm^3) at room temperature for 2 hours. The resulting black reaction mixture was filtered off over a sintered funnel and the precipitate was rinsed with dichloromethane (10 cm^3). Evaporation of the filtrate afforded a pale yellowish oily product which was identified as *N,N′*-diphenylcarbodiimide (**6**) (0.32 g, 95%). The product was used without further purification.

4-Amino-6-phenylamino-2-phenylimino-1-phenyl-1,2-dihydro-1,3,5-triazine (1)

Guanidine to N,N′-diphenylcarbodiimide molar ratio = 1 : 2. To a solution of *N,N′*-diphenylcarbodiimide (**6**), (0.98 g, 5.0 mmol, prepared as previously described) in dry THF (10 cm^3) guanidine (**4**) (0.15 g, 2.5 mmol) was added and the reaction mixture was heated under reflux for 24 hours. The pale yellowish crude mixture remaining upon the removal of the solvent was suspended in acetonitrile (10 cm^3), the precipitated white solid was filtered off, washed with cold acetonitrile (5 cm^3) and dried in air (0.45 g, 51%). Evaporation of the filtrate yielded a yellow residue, which was suspended in 3.0 cm^3 of acetonitrile. The crystals that precipitated were separated by filtration and washed with 2.0 cm^3 of cold acetonitrile, affording 0.53 g (60%) of product **1** in total.

Guanidine to N,N′-diphenylcarbodiimide molar ratio = 1 : 3. To a solution of *N,N′*-diphenylcarbodiimide (**6**), (0.314 g, 1.6 mmol, prepared as previously described) in dry THF (3 cm^3) guanidine (**4**) (0.031 g, 0.53 mmol) was added and the mixture was refluxed for 24 hours. The crude reaction mixture remaining upon the removal of the solvent was first suspended in diethylether (5 cm^3), the precipitated white solid was filtered off and then again suspended in acetonitrile (2 cm^3), followed by filtration and additional washing with acetonitrile (2 cm^3). The solid was dried in air to afford pure dihydrotriazine **1** (0.184 g, 98%).

Evaporation of the filtrate afforded a pale yellowish residue as a mixture of *N,N′*-diphenylbiguanide (∼8%) and *N,N′*, *N′′*-triphenylguanidine (**8**) (∼92%, by HPLC). An analytically pure sample of guanidine by-product **8** was obtained by the recrystallisation of the residue from ethanol.

A single crystal suitable for X-ray crystallographic measurement was obtained by dissolving a sample of **1** (0.10 g) in an ethanol–methanol 2 : 1 mixture (15 cm^3). After 4 days of slow evaporation, the product was crystallized in the form of colorless prisms (65 mg, 65%).

mp 277–278 °C (from EtOH–MeOH 2 : 1 mixture) (lit.,[1] 270–271 °C). Found: C, 70.0%; H, 5.4%; N, 23.0% $C_{21}H_{18}N_6 \cdot 0.5CH_3OH$ requires C, 69.7%; H, 5.45%; N, 22.7%. υ_{max}/cm^{-1} 3393, 3154, 1637, 1588, 1534, 1463, 1362, 1295, 1143, 772, 743, 700. δ_H(600 MHz; d_6-DMSO; Me_4Si) 6.40–7.40 (12 H, m, overlapped Ph and NH_2 protons), 7.44–7.46 (3 H, m, Ph), 7.52–7.55 (2 H, m, Ph), 7.61 (1 H, s, N*H*). δ_C(150 MHz, d_6-DMSO; Me_4Si) 119.5–121, 123–125 (br), 127.9, 128.4, 129.62, 129.64, 136.5, 162.4. HRMS-MALDI found: 355.1683; calc. for $C_{21}H_{19}N_6$ (MH^+): 355.1666.

4-Dimethylamino-6-phenylamino-2-phenylimino-1-phenyl-1,2-dihydro-1,3,5-triazine (2)

N,N-Dimethylguanidine to N,N′*-diphenylcarbodiimide molar ratio = 1 : 2*. To a solution of *N,N′*-diphenylcarbodiimide (**6**),

(1.01 g, 5.2 mmol) in dry THF (10 cm^3) *N*,*N*-dimethylguanidine (**5**) (0.22 g, 2.5 mmol, prepared as previously described) was added and the reaction mixture was heated under reflux for 24 hours. The mixture of yellow oil and solid remaining upon removal of the solvent was removed and the residue suspended in diethylether (5 cm^3). The precipitated white solid was filtered off and washed with ether (0.44 g, 46%). Evaporation of the filtrate produced yellow oil, which solidified upon standing at room temperature (0.83 g, contains approximately 12% of the product according to HPLC analysis). Subsequent crystallization from the mother liquor afforded an additional 0.05 g of product **2**, thus increasing the yield to 51%.

N,N-Dimethylguanidine to N,N′-diphenylcarbodiimide molar ratio = 1 : 3. To a solution of *N*,*N*′-diphenylcarbodiimide (**6**), (0.314 g, 1.6 mmol, prepared as previously described) in dry THF (3 cm^3) *N*,*N*-dimethylguanidine (**5**) (0.047 g, 0.53 mmol) was added and the mixture was refluxed for 24 hours. The crude reaction mixture remaining upon the removal of the solvent was suspended in diethylether (4 cm^3), the precipitated white solid was filtered off and dried in air to afford pure dihydrotriazine **2** (0.193 g, 94%).

Evaporation of the filtrate yielded a pale yellowish residue of *N*,*N*′,*N*″-triphenylguanidine (**8**) (>95% by HPLC analysis, crude product yield 97%).

A single crystal suitable for X-ray crystallographic studies was obtained by dissolving a sample of **2** (0.10 g) in methanol (8.0 cm^3). The product crystallized in the form of pale yellowish prisms (66 mg, 66%).

mp 197–198 °C (from MeOH). Found: C, 71.4%; H, 5.7%; N, 21.9% $C_{23}H_{22}N_6$ requires C, 72.2%; H, 5.8%; N, 22.0%. υ_{max}/cm^{-1} 3390, 2923, 2853, 1629, 1611, 1584, 1534, 1487, 1467, 1401, 1218, 765, 694. δ_H(600 MHz; d_6-DMSO; Me_4Si) 2.97 (6 H, s, C*H*$_3$), 6.60–7.60 (15 H, m, overlapped Ph protons), 7.75 (1 H, s, N*H*). δ_C(150 MHz, d_6-DMSO; Me_4Si) 35.7, 120, 123, 124, 127.7, 128.5, 129.58, 129.63, 136.3, 137, 150, 151, 155, 160.0. HRMS-MALDI found: 383.1971; calc. for $C_{23}H_{23}N_6$ (MH^+): 383.1979.

4-Dimethylamino-6-phenylamino-2-phenylimino-1-phenyl-1,2-dihydro-1,3,5-triazinium perchlorate ((2·$HClO_4$). A sample of **2** (0.10 g, 0.26 mmol) was dissolved in methanol (5 cm^3), followed by the addition of 1 mol dm^{-3} perchloric acid (261 μL, 0.26 mmol). The mixture was evaporated and the remaining solid was suspended in water (2.5 cm^3). The suspension was gently heated and ethanol was added until the solution became clear. The solution was left overnight at room temperature and the precipitated colorless needle-like crystals of the triazine perchlorate salt **2**·$HClO_4$ were filtered off and dried in air (0.09 g, 74%).

mp 203–205 °C (from H_2O–EtOH mixture). υ_{max}/cm^{-1} 3402, 3063, 2930, 1657, 1622, 1589, 1543, 1462, 1411, 1225, 1120, 1095, 764, 745, 722, 692, 623, 561. δ_H(600 MHz; d_6-DMSO; Me_4Si) 3.01 (6 H, s, C*H*$_3$), 7.22–7.27 (2 H, m, Ph), 7.32–7.41 (8 H, m, Ph), 7.70–7.84 (5 H, m, Ph), 8.81 (2 H, s, N*H*). δ_C(150 MHz, d_6-DMSO; Me_4Si) 36.1, 125.7, 126.1, 128.1, 129.4, 130.8, 131.62, 131.64, 136.3, 154.1, 159.9.

***N*,*N*′,*N*″-Triphenylguanidine (8)**. mp 150–151 °C (from EtOH). υ_{max}/cm^{-1} 3384, 3015, 1630, 1581, 1542, 1494, 1436, 1319, 1253, 750, 734, 692. δ_H(600 MHz; d_6-DMSO; Me_4Si) 6.71–6.82 (5 H, m, Ph), 6.97–7.30 (10 H, m, Ph), 8.23 (2 H, s, N*H*). δ_C(150 MHz, d_6-DMSO; Me_4Si) 118.2 (br), 120.7, 121.7 (br), 128.4, 141.6 (br), 144.9.

4-Dimethylamino-6-isopropylamino-2-isopropylimino-1-isopropyl-1,2-dihydro-1,3,5-triazine (3). A solution of *N*,*N*-dimethylguanidine (**5**) (0.87 g, 0.01 mol) and *N*,*N*′-diisopropyl-carbodiimide (**7**) (3.15 cm^3, 0.02 mol) in dry THF (50 cm^3) was heated under reflux for 24 hours. The solvent was evaporated and the pale yellowish residue subjected to high vacuum distillation. The unreacted carbodiimide **2** was removed at room temperature and pressure of 2×10^{-4} mbar, while the main product was distilled at the same pressure and 130 °C as viscid colorless oil, which solidified upon cooling in a refrigerator (2.23 g, 80%).

mp 42–43 °C. υ_{max}/cm^{-1} 3301, 3214, 2969, 2931, 2874, 1602, 1565, 1547, 1491, 1410, 1168, 778. δ_H(600 MHz; d_6-DMSO; Me_4Si) 0.96 (6 H, d, *J* 6.3, $(CH_3)_2CH$), 1.17 (6 H, d, *J* 6.6, $(CH_3)_2CH$), 1.41 (6 H, d, *J* 6.8, $(CH_3)_2CH$), 2.96 (6 H, s, C*H*$_3$), 3.96–4.03 (1 H, m, $(CH_3)_2CH$), 4.16–4.24 (1 H, m, $(CH_3)_2CH$), 4.68–4.76 (1 H, m, $(CH_3)_2CH$), 6.15 (1 H, d, *J* 7.2, N*H*). δ_C (150 MHz, d_6-DMSO; Me_4Si) 19.4, 22.1, 24.5, 35.5, 42.8, 45.0, 45.3, 148.2, 155.1, 159.2. HRMS-MALDI found: 281.2437; calc. for $C_{14}H_{29}N_6$ (MH^+): 281.2448.

4-Dimethylamino-2,6-*bis*(isopropylamino)-1-isopropyl-1,3,5-triazinium perchlorate (3·$HClO_4$). A sample of **3** (0.52 g, 1.85 mmol) was dissolved in a mixture of methanol (6 cm^3) and 1 mol dm^{-3} perchloric acid (1.85 cm^3, 1.85 mmol). The solution was left overnight at room temperature, the colorless crystals of the triazine perchlorate salt **3**·$HClO_4$ were filtered off and dried in air (0.48 g, 68%).

mp 178–179 °C (from MeOH). Found: C, 44.15%; H, 7.25%; N, 21.4% $C_{14}H_{29}N_6O_4Cl$ requires C, 44.15%; H, 7.7%; N, 22.05%. υ_{max}/cm^{-1} 3215, 2969, 1607, 1559, 1453, 1411, 1166, 1140, 1118, 1087, 778, 627. δ_H(300 MHz; d_6-DMSO; Me_4Si) 1.24 (12 H, d, *J* 6.6, $(CH_3)_2CH$), 1.49 (6 H, d, *J* 7.0, $(CH_3)_2CH$), 3.12 (6 H, s, C*H*$_3$), 4.27–4.40 (2 H, m, $(CH_3)_2CH$), 4.51–4.64 (1 H, m, $(CH_3)_2CH$), 7.13 (2 H, d, *J* 7.5, N*H*). δ_C(75 MHz, d_6-DMSO; Me_4Si) 19.1, 21.3, 36.1, 44.7, 48.7, 153.5, 159.3.

X-Ray structure determination

Crystallographic data were collected on an Oxford Diffraction Xcalibur CCD diffractometer with graphite-monochromated Mo Kα radiation at low temperature (Table 3) and room temperature (only for **2**, Table S7 in ESI†). The programs CrysAlis CCD and CrysAlis RED[27] were used for data collection, cell refinement and data reduction. The structure was solved by direct methods. A refinement procedure by full-matrix least squares methods based on F^2 values against all reflections included anisotropic displacement parameters for all non-H atoms. The positions of hydrogen atoms were geometrically optimized applying the riding model except in **1**·0.5 MeOH where they were found in the difference Fourier map and isotropically refined (only those on MeOH were geometrically optimized). Calculations were performed with SHELXS97[28] and SHELXL97[29] (both operating under the WinGX[30] program package). The molecular graphics were

done with PLATON98[31] and Mercury.[32] Supplementary crystallographic data sets for the structures **1**·0.5 MeOH, **2** (at low and room temperature), **2**·$HClO_4$ and **3**·$HClO_4$ are available through CCDC 830994–830998.

pK_a determination

The UV-Vis spectrophotometric titration method used in this work was described in detail in ref. 20*a*, *c*, and *d*. For each investigated compound, the relative acidity and basicity were measured against at least two (mostly three) different reference compounds with known pK_a values in AN.[20a,b,d] To determine the relative acidity of two compounds, a mixture of two different acids was titrated with UV-Vis radiation non-absorbing acidic and basic titrants to obtain several spectra of solutions containing both neutral and anionic forms of the two acids in different proportions. Both of the acids were also titrated separately to obtain the spectra of the neutral and anionic forms of the pure compounds. The relative basicities were determined in a similar way, although in this case the solutions contained neutral and cationic forms. From the titration data, the relative acidity of the acids or the relative acidity of the conjugate acids of the bases—the difference between the pK_a values (ΔpK_a values)—was calculated (see ref. 20*a*, *c*, *d*). During titrations, the protonation–deprotonation processes were reversible with all the compounds and sharp isosbestic points (at which the absorption of neutral and ionic forms are the same) were obtained. All the compounds investigated in this work have significantly different spectra of protonated and deprotonated forms in the UV region (major changes between 250–300 nm for **1** and 250–350 nm for **2** and **3**) and calculation methods using only spectral data obtained from the titration of pure compounds and mixture were used to obtain ΔpK_a values. From the ΔpK_a values of measurements carried out in this work and from the absolute pK_a values assigned to the reference compounds in previous works,[20a,b,d] the absolute pK_a values of the investigated compounds were obtained as the average of absolute values. From each titration experiment of the mixture of two compounds, the ΔpK_a value was determined as the mean of 10–20 values. Concentrations of the measured compounds were mostly in the order of $n \cdot 10^{-5}$ M and never exceeded 2×10^{-4} M, while concentrations of acidic and basic titrants were in the 3×10^{-3} M range.

Quantum chemical calculations

Quantum calculations were carried out with the GAUSSIAN-03 program package[33] using Becke's three-parameter exchange functional with the correlation functional of Lee, Yang and Paar (B3LYP).[34] Geometries were fully optimized with the 6-31G(d) valence double ξ-basis set of Pople and Hariharan, and were confirmed to be minima by computing their analytical vibrational frequencies. Single-point calculations were then performed with the 6-311+G(d,p) basis set. The zero point vibrational energies computed at the B3LYP/6-31G(d) level used in the proton affinity calculations are unscaled. Proton affinities are calculated at the B3LYP6-311+G(d,p)//B3LYP/6-31G(d) level employing the general equation: PA(B) = (ΔE_{el}) + (ΔZPVE), where (ΔE_{el}) = [E(B) − E(BH^+)] and (ΔZPVE) = [ZPVE(B) − ZPVE(BH^+)] are the electronic and the zero-point vibrational energy contributions to the proton affinity, respectively. Here, B and BH^+ denote the base in question and its conjugate acid, respectively. Solvation energies were calculated at the IEF-PCM/HF/6-31G(d) level of theory using radii optimized for COSMO-RS[35] for cavity construction. All the calculations were performed using the Gaussian 03 program package with default parameters.

Acknowledgements

Financial support of this work by the Ministry of Science, Education and Sports of Croatia (Project No. 098-0982933-2920 (M.E.-M.) and 119-119079-1084 (D.M.-Č.) is acknowledged. The work of I. L. and J. S. was supported by Grant No. 7374 from the Estonian Science Foundation. We also thank Dr Z. Glasovac for assistance in calculations of basicities and Dr Mario Cindrić (Center for Proteomics and Mass Spectrometry, Rudjer Bošković Institute) for HRMS analyses.

References

1 (*a*) S. Mehrotra, V. Pandey, R. Lakhan and P. K. Srivastava, *J. Indian Chem. Soc.*, 2002, **79**, 176; (*b*) P. Mamalis, *Ger. Offen.*, 1934, **120**, 1970.
2 A. Gopalsamy and H. Y. Yang, *US Pat. Appl.*, 49,320, 2002.
3 (*a*) T. Vilaivan, N. Saesaengseerung, D. Jarprung, S. Kamchonwongpaisan, W. Sirawaraporn and Z. Yuthavong, *Bioorg. Med. Chem.*, 2003, **11**, 217; (*b*) P. Mamalis and D. J. Outred, *Ger. Offen.*, 1,957,769, 1970; (*c*) P. Mamalis and D. J. Outred, *Ger. Offen.*, 1,965,711, 1970; (*d*) P. Mamalis, *Ger. Offen.*, 1,963,759, 1970; (*e*) A. Nzila, *J. Antimicrob. Chemother.*, 2006, **57**, 1043.
4 G. Moinet, D. Cravo, L. Doare, M. Kergoat and D. Mesangeau, *PCT Int. Appl.*, WO 01 55 122, 2001.
5 S. Hayashi, M. Furukawa, J. Yamamoto, Y. Nishizima, E. Sannomiya and H. Ueki, *Kumamoto Pharm. Bull.*, 1966, **7**, 7.
6 (*a*) M. D. Turnbull, P. J. Crowley, E. J. T. Chrystal, J. M. Clough, I. B. Bryan, K. Beautement, S. P. Barnett, R. J. Ponsford and D. J. Outred, *PCT Int. Appl.*, WO 9615671, 1966; (*b*) R. Smrz, J. Cech, J. Auerhan and A. Simek, *Czech Patent*, 119,884, 1966.
7 (*a*) C. J. Peake and S. Y. Lin, *Patent US*, 5,565,451; (*b*) C. J. Peake, T. G. Cullen and A. C. Lew, *Patent US*, 5,300,503, 1994.
8 (*a*) A. Kummar, S. K. Patnaik and M. M. Singh, *Mater. Chem. Phys.*, 1998, **56**, 243; (*b*) M. M. Singh and A. Gupta, *Bull. Electrochem.*, 1996, **12**, 511.
9 (*a*) A. Rosowsky, K. K. N. Chen, R. St. Amand and E. J. Modest, *J. Pharm. Sci.*, 1973, **62**, 477; (*b*) E. Rossi, G. Abbiati and D. Nava, *Heterocycles*, 1999, **51**, 1401; (*c*) G. Lowe, C. Carr and R. Quarrell, *Chem. Commun.*, 2001, 737; (*d*) H.-K. Lee and T. M. Rana, *J. Comb. Chem.*, 2004, **6**, 504; (*e*) M. Kidwai, P. Mothsra, R. Mohan and S. Biswas, *Bioorg. Med. Chem. Lett.*, 2005, **15**, 915; (*f*) M. V. Vovk, A. V. Bol'but, P. S. Lebed and N. V. Mel'nichenko, *Zh. Org. Khim.*, 2007, **43**, 929; (*g*) D. Gravestock, A. L. Rousseau, A. C. U. Lourens, S. S. Moleele, R. L. Van Zyl and P. A. Steenkamp, *Eur. J. Med. Chem.*, 2011, **46**, 2022.
10 (*a*) Z. Glasovac, B. Kovačević, E. Meštrović and M. Eckert-Maksić, *Tetrahedron Lett.*, 2005, **46**, 8733; (*b*) A. Tintaru, J. Roithová, D. Schröder, L. Charles, I. Jušinski, Z. Glasovac and M. Eckert-Maksić, *J. Phys. Chem. A*, 2008, **112**, 12097; (*c*) Z. Glasovac, V. Štrukil, M. Eckert-Maksić, D. Schröder, M. Kaczorowska and H. Schwarz, *Int. J. Mass Spectrom.*, 2008, **270**, 39; (*d*) Z. Glasovac, V. Štrukil, M. Eckert-Maksić, D. Schröder, M. Schlangen and H. Schwarz, *Int. J. Mass Spectrom.*, 2010, **291**, 22; (*e*) V. Štrukil, L. Fabian, D. G. Reid, M. J. Duer, G. J. Jackson, M. Eckert-Maksić and T. Friščić, *Chem. Commun.*, 2010, **46**, 9191.
11 F. Kurzer and E. D. Pitchfork, *J. Chem. Soc.*, 1964, 3459.
12 F. Kurzer and E. D. Pitchfork, *The Chemistry of Biguanides*, in *Fortschr. Chem. Forshung*, Springer Verlag, Berlin-Heidelberg, edn. 10/3, 1968, p. 375.

13 F. Kurzer and K. Douraghi-Zadeh, *Chem. Rev.*, 1967, **67**, 107.
14 (*a*) Z. Maksić and B. Kovačević, *J. Org. Chem.*, 2000, **65**, 3303; (*b*) B. Kovačević, Z. B. Maksić and R. Vianello, *J. Chem. Soc., Perkin Trans. 2*, 2001, 886; (*c*) K. Kovačević and Z. B. Maksić, *Chem.–Eur. J.*, 2002, **8**, 1694; (*d*) B. Kovačević, Z. Glasovac and Z. B. Maksić, *J. Phys. Org. Chem.*, 2002, **15**, 765.
15 See, *e.g.*, (*a*) R. E. Valters and W. Flitsch, *Ring–Chain Tautomerism*, ed. A. R. Katritzky, Plenum Press, New York, 1985; (*b*) R. E. Valters, F. Fülöp and D. Korbonits, *Adv. Heterocycl. Chem.*, 1995, **64**, 251; (*c*) R. E. Valters, F. Fülöp and D. Korbonits, *Adv. Heterocycl. Chem.*, 1996, **66**, 1–71.
16 (*a*) N. Hesse, R. Frölich, B. Wibbeling and E.-U. Würthwein, *Eur. J. Org. Chem.*, 2006, 3923; (*b*) M. Buhmann, M. H. Möller and E.-U. Würthwein, *Chem. Ber.*, 1993, **126**, 957; (*c*) M. Buhmann, M. H. Möller, U. Rodewald and E.-U. Würthwein, *Chem. Ber.*, 1993, **126**, 2467.
17 P. V. Gushchin, N. A. Bokach, K. V. Luzyanin, A. A. Nazarov, M. Haukka and V. Y. Kukushkin, *Inorg. Chem.*, 2007, **46**, 1684.
18 F. H. Allen, O. Kennard, D. G. Watson, L. Brammer, G. A. Orpen and R. Taylor, *J. Chem. Soc., Perkin Trans. 2*, 1987, S1.
19 M. Eckert-Maksić, Z. Glasovac, P. Trošelj, A. Kütt, T. Rodima, I. Koppel and I. A. Koppel, *Eur. J. Org. Chem.*, 2008, 5176.
20 (*a*) A. Kütt, I. Leito, I. Kaljurand, L. Sooväli, V. M. Vlasov, L. M. Yagupolskii and I. A. Koppel, *J. Org. Chem.*, 2006, **71**, 2829; (*b*) A. Kütt, V. Movchun, T. Rodima, T. Dansauer, E. B. Rusanov, I. Leito, I. Kaljurand, J. Koppel, V. Pihl, I. Koppel, G. Ovsjannikov, L. Toom, M. Mishima, M. Medebielle, E. Lork, G.-V. Röschenthaler, I. A. Koppel and A. A. Kolomeitsev, *J. Org. Chem.*, 2008, **73**, 2607; (*c*) I. Leito, I. Kaljurand, I. A. Koppel, L. M. Yagupolskii and V. M. Vlasov, *J. Org. Chem.*, 1998, **63**, 7868; (*d*) I. Kaljurand, A. Kütt, L. Sooväli, T. Rodima, V. Mäemets, I. Leito and I. A. Koppel, *J. Org. Chem.*, 2005, **70**, 1019; (*e*) L. Sooväli, I. Kaljurand, A. Kütt and I. Leito, *Anal. Chim. Acta*, 2006, **566**, 290; (*f*) E.-I. Rõõm, A. Kütt, I. Kaljurand, I. Koppel, I. Leito, I. A. Koppel, M. Mishima, K. Goto and Y. Miyahara, *Chem.–Eur. J.*, 2007, **13**, 7631; (*g*) V. Palm, *Tables of Rate and Equilibrium Constants of Heterocyclic Organic Reactions*, ed. VINITI, Moscow-Tartu, 1975–1985.
21 *e.g.*, (*a*) N. Uchida, A. Taketoshi, J. Kuwabara, T. Yamamoto, Y. Inoue, Y. Watanabe and T. Kanbara, *Org. Lett.*, 2010, **12**, 5242; (*b*) K. T. Leffek, P. Pruszynski and K. Thanapaalasingham, *Can. J. Chem.*, 1989, **67**, 590.
22 for more recent papers, see, *e.g.* Z.-K. Jia, D.-M. Du, Z.-Y. Zhou, A.-G. Zhang and R.-Y. Hou, *Chem. Phys. Lett.*, 2007, **439**, 374 and references cited therein.
23 (*a*) M. T. Cancès, B. Mennucci and J. Tomasi, *J. Chem. Phys.*, 1997, **107**, 3032; (*b*) S. Miertuš, E. Scrocco and J. Tomasi, *J. Chem. Phys.*, 1981, **55**, 117; (*c*) S. Miertuš and J. Tomasi, *J. Chem. Phys.*, 1982, **65**, 239.
24 (*a*) K. B. Wiberg, P. R. Rablen, D. J. Rush and T. A. Keith, *J. Am. Chem. Soc.*, 1995, **117**, 4261; (*b*) J. B. Foresman, T. A. Keith, K. B. Wiberg, J. Snoonian and M. J. Frisch, *J. Phys. Chem.*, 1996, **100**, 16098.
25 Z. Glasovac, M. Eckert-Maksić and Z. B. Maksić, *New J. Chem.*, 2009, **33**, 588.
26 Z. Glasovac, M. Eckert-Maksić and Z. B. Maksić, to be published.
27 Oxford Diffraction (2010). Oxford Diffraction Ltd., Xcalibur CCD system, CrysAlis Software system, Version 1.171.34.44.
28 (*a*) G. M. Sheldrick, *SHELXS, Program for the Solution of Crystal Structures*, University of Göttingen, Germany, 1997; (*b*) G. M. Sheldrick, *Acta Crystallogr.*, 2008, **A64**, 112.
29 (*a*) G. M. Sheldrick, *SHELXL97, Program for the Refinement of Crystal Structures*, University of Göttingen, Germany, 1997; (*b*) G. M. Sheldrick, *Acta Crystallogr.*, 2008, **A64**, 112.
30 L. J. Farrugia, *J. Appl. Crystallogr.*, 1999, **32**, 837.
31 C. F. Macrae, P. R. Edgington, P. McCabe, E. Pidcock, G. P. Shields, R. Taylor, M. Towler and J. van de Streek, *J. Appl. Crystallogr.*, 2006, **39**, 453.
32 A. L. Spek, *J. Appl. Crystallogr.*, 2003, **36**, 7.
33 M. J. Frisch, G. W. Trucks, H. B. Schlegel, G. E. Scuseria, M. A. Robb, J. R. Cheeseman, J. A. Montgomery Jr., T. Vreven, K. N. Kudin, J. C. Burant, J. M. Millam, S. S. Iyengar, J. Tomasi, V. Barone, B. Mennucci, M. Cossi, G. Scalmani, N. Rega, G. A. Petersson, H. Nakatsuji, M. Hada, M. Ehara, K. Toyota, R. Fukuda, J. Hasegawa, M. Ishida, T. Nakajima, Y. Honda, O. Kitao, H. Nakai, M. Klene, X. Li, J. E. Knox, H. P. Hratchian, J. B. Cross, C. Adamo, J. Jaramillo, R. Gomperts, R. E. Stratmann, O. Yazyev, A. J. Austin, R. Cammi, C. Pomelli, J. W. Ochterski, P. Y. Ayala, K. Morokuma, G. A. Voth, P. Salvador, J. J. Dannenberg, V. G. Zakrzewski, S. Dapprich, A. D. Daniels, M. C. Strain, O. Farkas, D. K. Malick, A. D. Rabuck, K. Raghavachari, J. B. Foresman, J. V. Ortiz, Q. Cui, A. G. Baboul, S. Clifford, J. Cioslowski, B. B. Stefanov, G. Liu, A. Liashenko, P. Piskorz, I. Komaromi, R. L. Martin, D. J. Fox, T. Keith, M. A. Al-Laham, C. Y. Peng, A. Nanayakkara, M. Challacombe, P. M. W. Gill, B. Johnson, W. Chen, M. W. Wong, C. Gonzalez and J. A. Pople, *Gaussian 03, Revision B.03*, Gaussian, Inc., Pittsburgh, PA, 2003.
34 (*a*) A. D. Becke, *J. Chem. Phys.*, 1993, **98**, 5648; (*b*) A. Schäfer, H. Horn and R. Ahlrichs, *J. Chem. Phys.*, 1992, **97**, 2571.
35 A. Klamt, V. Jonas, T. Buerger and J. C. W. Lohrenz, *J. Phys. Chem.*, 1998, **102**, 5074.

